Periodic vortex pinning with magnetic and nonmagnetic dots: The influence of size

A. Hoffmann
University of California–San Diego, Department of Physics 0319, La Jolla, California 92093-0319
and Manual Lujan Jr. Neutron Scattering Center, Los Alamos National Laboratory, Los Alamos, New Mexico 87545

P. Prieto* and Ivan K. Schuller
University of California–San Diego, Department of Physics 0319, La Jolla, California 92093-0319
(Received 11 October 1999)

Periodic pinning arrays can give rise to commensurability effects for the vortex pinning in superconductors. We studied the influence of size and separation of the individual pinning centers made out of magnetic and nonmagnetic dots. While there is some dependence on the dot size, the periodic pinning changes its character drastically, as soon as the separation between dots becomes comparable to the coherence length of the superconductor. This can be understood by a crossover from a weak pinning regime to a superconducting wire network regime with decreasing dot separation. In addition, the comparison between the periodic pinning of magnetic dot arrays and nonmagnetic dot arrays shows that the former generally show more pronounced periodic pinning. This indicates conclusively a magnetic contribution to the pinning mechanism.

I. INTRODUCTION

Vortices in type-II superconductors exhibit a wide variety of interesting physics. The interaction of the vortices with each other and with pinning centers in the superconductor gives rise to a rich variety of static and dynamic phases.[1–3] The use of artificial pinning centers allows for a detailed study of these various phases. In particular, the use of regular arrays of pinning centers such as thickness modulations,[4] holes,[5,6] or magnetic dots[7–9] gives rise to new commensurability effects, which gives additional insight into the elastic and pinning properties of vortices.[10]

New lithographic techniques allow the fabrication of artificial pinning arrays, where the size of each pinning center and their separations are comparable to the superconducting coherence length ξ and magnetic penetration depth λ.[6,8] This generated renewed experimental[6,8,11–13] and theoretical[14–18] interest into periodic vortex pinning. Studying the periodic vortex pinning in superconductors with arrays of holes showed that sufficiently large holes can stabilize multiquanta vortices[6,19,20] and that the optimal size for a hole as a pinning center can be considerably larger than the coherence length ξ.[21] It also has been suggested theoretically that the optimal size of a pinning center is related to λ instead of ξ.[22,23]

Here we investigate the effect of magnetic dot size on the periodic pinning, in contrast to earlier experiments which used holes (''antidots'') in the superconductor as pinning centers.[6,19–21] Compared with the antidots, the role of the pinning center size may be more complex for the magnetic dots, since there are various possible mechanisms by which they can give rise to vortex pinning.[7–9,24] To clarify this further, we also compare the results with magnetic and nonmagnetic dots.

The paper is organized as follows: In Sec. II we describe the sample preparation and measurements. Following this, the results for samples with different sized magnetic dots are presented and discussed in Sec. III. Subsequently in Sec. IV, these results are compared to samples with nonmagnetic dots.

II. EXPERIMENT

The fabrication of small magnetic structures (''dots'') using *e*-beam lithography has been described in detail in Ref. 25. Briefly, *e*-beam lithography is used to define the desired structure into an electron sensitive resist (PMMA) which is coated on top of a Si (100) substrate. During the *e*-beam lithography the size of the dots is controlled by varying the electron beam dosage between 0.4 and 6 nC/cm. Following the e-beam lithography the material of choice for the dots (Ni for magnetic dots, Ag for nonmagnetic dots) is deposited using dc magnetron sputtering. A final lift-off step removes the unwanted material together with the remaining PMMA. For the samples discussed in this paper, the dots are 34–41 nm thick, have a diameter between 100 and 530 nm, and cover an area of $50\times50\ \mu m^2$. One series of Ni dots is shown in Fig. 1.

To determine the role of dot size for the periodic pinning we tried to eliminate any possible extrinsic influences. Therefore we prepared several series of samples where the deposition of the dot material (Ni or Ag) and the superconducting Nb, as well as any other processing steps were done simultaneously. Thus (hopefully) the only varying parameter for each sample in each series is the dot diameter.

After the dots are fabricated, they are covered with a superconducting Nb film deposited in a molecular beam epitaxy (MBE) system. Next, a standard four-point measurement bridge is defined photolithographically in the Nb film such that the Nb transport properties are measured where it covers the dots or is in direct contact with the substrate. The transport measurements are performed in a He flow cryostat with a 9-T magnet. Since most measurements were done very close to the superconducting critical temperature T_c, the temperature was stabilized within ±2 mK during the

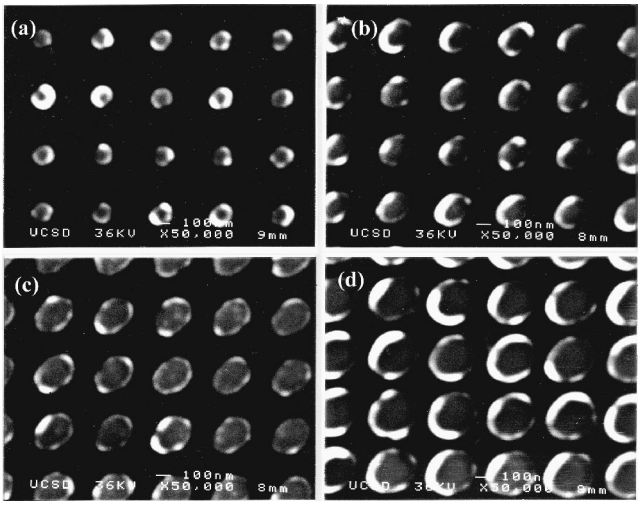

FIG. 1. Scanning electron micrograph of Ni dots with different diameters [(a) 110, (b) 180, (c) 270, and (d) 340 nm]. The scale for all the pictures is the same and is given at the bottom of each picture.

measurements to avoid any significant contribution of thermal noise. $I(V)$ curves were measured using a dc setup for determining the critical current density. Due to the small dimensions of the measurement bridge of 50×40 μm^2 we used a voltage criterion of 20 μV/cm (corresponding to 0.1 μV in the sample, with a signal to noise of 10) to determine critical currents.

III. MAGNETIC DOTS

A. Results

In Fig. 2 we show the magnetoresistance ρ for four samples consisting of 56-nm thick Nb films covering different sized Ni dots, ranging in diameter from 110 to 340 nm

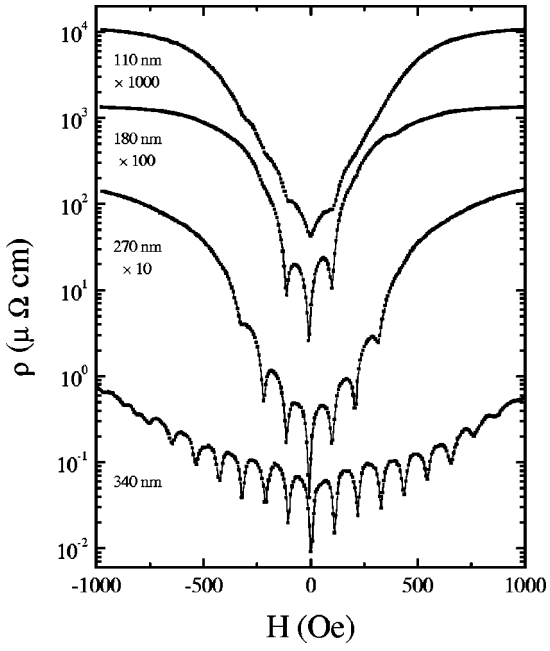

FIG. 2. $\rho(H)$ for samples with different Ni dot diameter d. The curves are shifted by factors of 10 from each other.

(the actual dots are shown in Fig. 1) and having a thickness of 34 nm. Clearly magnetoresistance minima are observed for all samples at equidistant magnetic field intervals. These minima in the magnetoresistance have been previously explained by a geometric matching between the vortex lattice and the magnetic dot array, which gives rise to a periodic pinning potential.[8] The position of these peaks can be easily determined from the geometry of the pinning array and is given in the case of a square array by[5,26]

$$H_n=\frac{\Phi_0}{a^2}, \tag{1}$$

where H_n is the so-called nth matching field, $\Phi_0=20.7$ G/μm^2 is the flux quantum (the magnetic flux in each vortex), and a is the lattice parameter of the square pinning array. Thus at H_n there are exactly n vortices per pinning center. For all four samples, the Ni dots were arranged on a square lattice with a lattice constant of 400 nm, thus the matching peaks occur for all samples at the same magnetic fields. Furthermore the position of the matching peaks in Fig. 2 are in good agreement with the theoretically expected positions calculated from Eq. (1).

Figure 2 shows that the periodic pinning becomes much more pronounced for larger magnetic dots. The number and depth of matching peaks increases with increasing dot diameter. This observation is generally true independent of measurement temperature or current density. However, for better comparison, the measurements shown in Fig. 2 were taken with the temperature adjusted for each sample such that the critical current density at zero magnetic-field was 30–80 kA/cm^2. The current for the measurement was then chosen to be twice the critical current density at zero magnetic field. This gives rise to the most pronounced pinning peaks in all samples.

The changes of the magnetoresistance as a function of Ni dot diameter are gradual. However, the magnetic-field dependence of the critical current density j_c (see Fig. 3) shows that the behavior of the sample with the largest (340 nm) Ni dots is qualitatively different than that with smaller dots. Periodic critical current density matching peaks are only observed for the largest Ni dots, while the matching peaks are absent for any of the smaller ones.

This pronounced difference between the sample with 340-nm diameter Ni dots and the samples with smaller Ni dot diameters is also reflected in the current-voltage $j(V)$ characteristics. This is shown in Fig. 4 for the samples with 340-nm Ni dots (a) and 270-nm Ni dots (b). Obviously the matching effects persist over the whole current-density range for the sample with 340 nm Ni dots [see Fig. 4(a)]. On the other hand, for the sample with 270-nm Ni dots there are no matching effects at low current densities and the matching effects occur only at higher current densities [see Figure 4(b)]. This is clearly indicated by the crossover of the $j(V)$ curves at a matching field (solid symbols) with the $j(V)$ curves just below the respective matching field (open symbols). Notice that this crossover occurs always at those current densities, at which the $j(V)$ curves show a very distinctive ''kink'' (i.e., a change in slope). The $j(V)$ curves obtained for the samples with 110- and 180-nm Ni dots are qualitatively similar to the ones shown in Fig. 4(b) for the sample with 270-nm Ni dots.

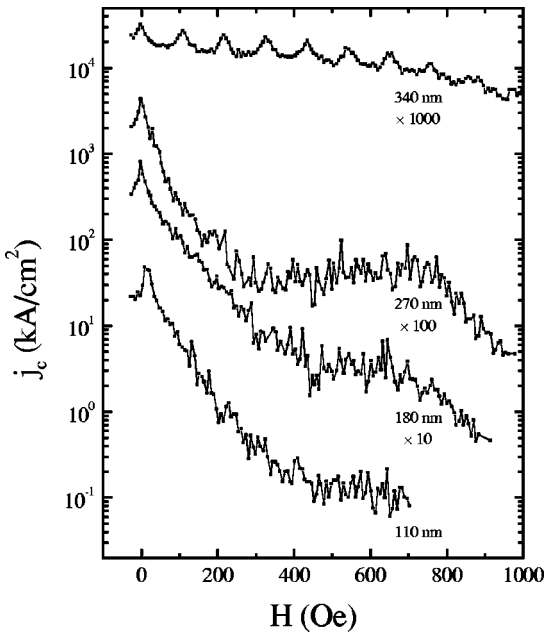

FIG. 3. $j_c(H)$ for samples with different Ni dot diameter d. The curves are shifted by factors of 10 from each other.

Figures 3 and 4 show that at low current densities the samples with the 340-nm Ni dots exhibit different behavior than the samples with the smaller Ni dots. Moreover, even at higher current densities, where all samples show periodic matching peaks in the magnetoresistance, there is a qualitative difference in the periodic pinning between these samples. This is shown in Fig. 5, where the normalized resistivity change $\Delta\rho/\rho$ at each matching field is shown for various current densities. For the sample with 340 nm Ni dots $\Delta\rho/\rho$ decreases monotonically with increasing matching field order n and increasing current density [see Fig. 5(a)]. In contrast, $\Delta\rho/\rho$ for the sample with 270-nm Ni dots shows for every matching field order n a maximum as a function of current density and also for most current densities as a function of n. Again, the samples with 110- and

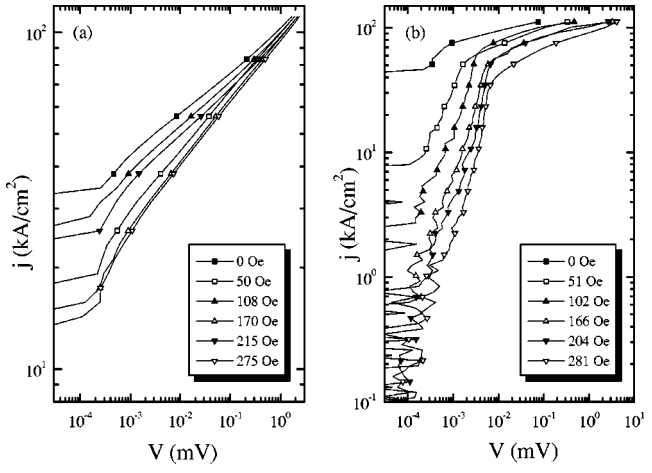

FIG. 4. $j(V)$ for samples with (a) 340-nm and (b) 270-nm Ni dots measured with different applied magnetic fields. Data taken at the minima of the $\rho(H)$ curves in Fig. 2 are shown with solid symbols, while data taken at the maxima of the $\rho(H)$ curves are shown with open symbols.

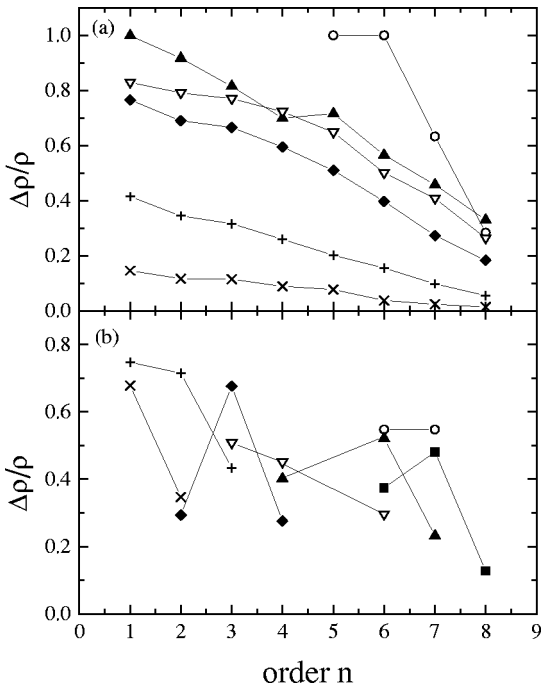

FIG. 5. $\Delta\rho/\rho$ as a function of matching field for samples with (a) 340-nm and (b) 270-nm Ni dots for different applied current densities (■ 4.5, o 11, ▲ 22, ▽ 33, ◆ 45, + 67, and × 89 kA/cm^2).

180-nm dots show qualitatively similar behavior to the one of the sample with 270-nm Ni dots shown in Fig. 5(b).

By now it is clearly established that the sample with 340-nm Ni dots shows different periodic pinning than the ones with smaller Ni dots. However, besides the increase in size there is also a decrease in the separation of the dots, since for all samples the lattice constant for the magnetic dot array is kept constant. Thus it is *a priori* not clear if the enhancement of the periodic pinning observed for the largest Ni dots is due to their size or their separation. In order to clarify this point, we prepared another series of 1070-Å-thick Nb films covering Ni dot arrays with a larger lattice constant, $a = 600$ nm. Figure 6 shows the magnetoresistance for two of these samples; one with 530-nm Ni dots (lower curve) and the other one with 400-nm Ni dots (upper curve). Clearly,

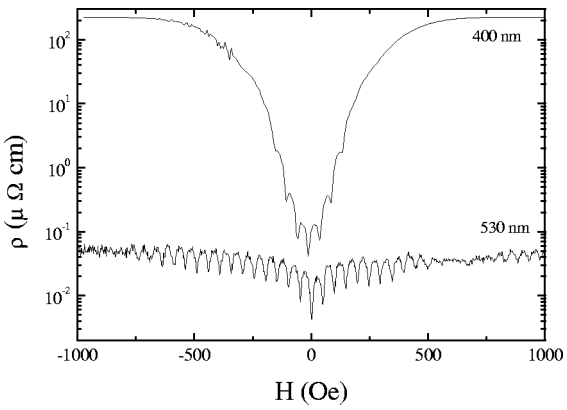

FIG. 6. $\rho(H)$ for samples with different Ni dot diameters d and a square array with $a = 600$ nm. The curve for the 400-nm Ni dots is shifted by a factor of 10.

the sample with the bigger dots shows many more matching peaks (up to 35th order with some intermediate peaks missing; this is not shown in Fig. 6). More importantly for the sample with 400-nm Ni dots on a 600-nm square array (see Fig. 6, upper curve) the matching effects are much less pronounced than for the sample with 340-nm Ni dots on a 400-nm square array (see Fig. 2, lowest curve). This unambiguously shows that the dot separation and not the dot size is responsible for the strong enhancement of the periodic pinning effects.

B. Discussion

The motivation for measuring the matching effects as a function of dot size was to investigate whether there is an optimal size of the dots for the vortex pinning. Generally, it is assumed that the optimal size of a pinning center is comparable to the size of the vortex core which has a diameter of approximately two times the coherence length ξ. By contrast, recent theoretical calculations suggest that the optimal pinning center size is comparable to the magnetic penetration depth λ.[22,23] Indeed, some recent experimental results suggest that the relevant length scale is larger than ξ for the pinning of vortices in superconductors with periodic arrays of holes.[21]

We determined for all our samples the temperature-dependent coherence length $\xi(T)$ from the upper critical field defined at 90% of the normal-state resistance. All samples with Ni, Ag, or without dots show exactly the same temperature dependence of the coherence length with an extrapolated zero-temperature value of $\xi = 9.5 \pm 0.1$ nm. Assuming that the coherence length reduction with respect to bulk Nb ($\xi = 38$ nm) (Ref. 27) is due to impurities in the thin films, we can deduce a zero-temperature magnetic penetration depth for our samples of $\lambda = 156 \pm 2$ nm.[24] At a typical measurement temperature of $T/T_c = 0.98$, the values for the coherence length and the magnetic penetration depth are $\xi \cong 58$ nm and $\lambda \cong 560$ nm, respectively. Thus for all our samples, the dot diameter exceeds the coherence length ξ and as a result one would not expect any change in the periodic pinning, if the optimal size of the pinning center would be given by ξ. Therefore our results are consistent with the view that the magnetic penetration depth λ may be the more important length scale for the vortex pinning.

On the other hand, an important result from the experiments presented here is that the nature of the periodic pinning changes drastically as soon as the separation between the dots becomes very small. For the sample with 340-nm Ni dots on a 400-nm square array the edge-to-edge distance between the dots is 60 nm, which is comparable to the coherence length ($\xi \approx 58$ nm) in the Nb films at the measurement temperature. This crossover in the pinning behavior when the separation of individual pinning centers becomes comparable to the coherence length, has also been observed earlier by V. V. Moshchalkov *et al.* for superconductors with arrays of holes.[21] Their explanation for this crossover was that if the separation between the pinning centers becomes comparable to the coherence length then the sample starts behaving effectively like a superconducting wire network. In this case, the lateral dimensions of the superconducting material in between the pinning center are too small to accommodate a vortex. As a result, each individual loop of the superconducting network (around each pinning center) will only contain a quantized magnetic flux and the whole network shows periodic oscillations of $T_c(H)$ [and hence of $\rho(H)$], which are reminiscent of Little-Parks oscillations.[28,29] However, for the arrays with smaller pinning centers the system is better described by a weak pinning of the vortices and the observed oscillatory peaks in the magnetoresistance are due to a geometric matching of the vortex lattice with the regular pinning array.[21]

More evidence that the samples with the smaller Ni dots are indeed described better with a weak pinning picture is given by the $j(V)$ curves shown in Fig. 4(b). As mentioned earlier, for these samples the matching effects are absent at low current densities but occur at current densities above a well defined kink in the $j(V)$ curves. Such a change in the $j(V)$ curves has been explained previously by a current induced ordering of the vortex lattice.[30] This is consistent with the negative curvature of the $j(V)$ curve just before the kink, since an increased ordering of the vortex lattice should result in a more effective pinning of the vortex lattice and hence in a reduction of the resistance. This current induced ordering of the vortex lattice can also explain the sudden onset of the matching effects observed at the kink in the $j(V)$ curves and is consistent with earlier measurements by J. I. Martín *et al.*[8]

IV. NONMAGNETIC DOTS

A. Results

For all the samples discussed in this paper and in our earlier works[8,10,26] the Nb film was always deposited on top of the magnetic dots. Consequently the Nb film has a periodic corrugation due to the dots. Naturally the question arises, whether pinning of the vortices is due to (i) a magnetic interaction of the vortices with the dots, or (ii) due to the structural corrugation of the Nb film. To discriminate between the two, a series of samples was prepared with nonmagnetic Ag dots. The samples consisted of 580-Å-thick Nb films covering 34-nm-thick Ag dots ranging in diameter from 100 to 300 nm; thus these samples can be easily compared to the first series of samples with Ni dots discussed in Sec. III since both the Nb film and the dot thicknesses are practically identical.

Figure 7 shows the magnetoresistance for the samples with different Ag dot diameters. For all samples there are clear first-order matching peaks. As in the samples with Ni dots (see Fig. 2), the samples with bigger dots show matching peaks up to higher orders, but generally for all samples with Ag dots there are less peaks, than for comparable samples with Ni dots. Notice also that the first-order matching peaks are much more pronounced than the peaks at higher orders.

The $j(V)$ curves for all samples with Ag dots are qualitatively similar and as an example we show the ones for the sample with 300-nm Ag dots in Fig. 8. As can be seen only for the first matching field there is a crossover for the $j(V)$ curves and also an enhancement of the critical current density, while the periodic pinning effects at the second matching field do not show up in these data. Thus the matching effects are most pronounced at the first matching field. Notice also that for the magnetic fields above the first matching

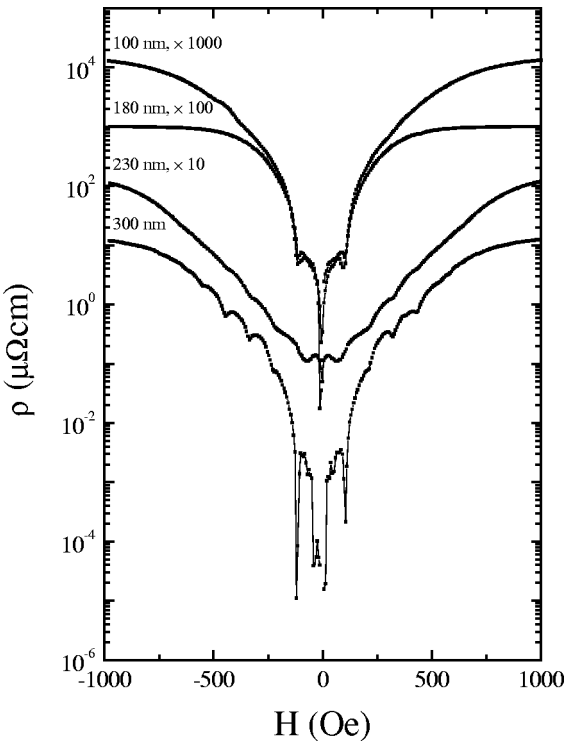

FIG. 7. $\rho(H)$ for samples with different Ag dot diameter d. The curves are shifted by factors of 10 from each other.

field the critical current density drops very rapidly and the $j(V)$ curves have two regions with different slopes. Interestingly the $j(V)$ curves for the samples with Ag dots are different from the $j(V)$ curves for the samples with the 340-nm

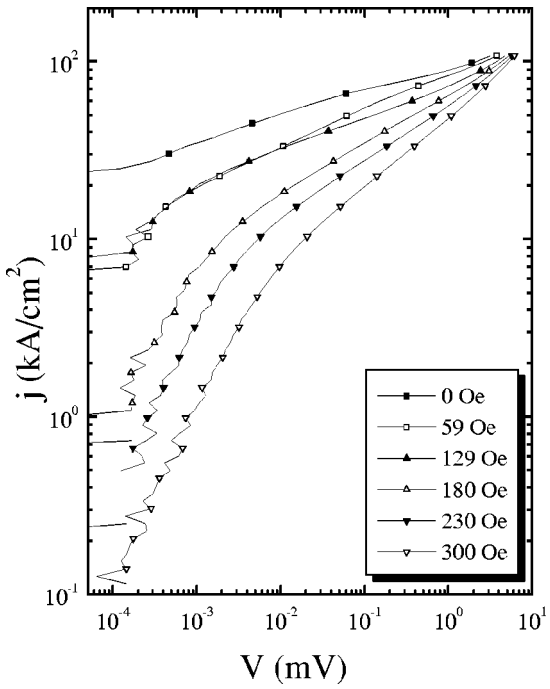

FIG. 8. $j(V)$ for the sample with 300-nm Ag dots measured with different applied magnetic fields. Data taken at the minima of the $\rho(H)$ curves in Fig. 7 are shown with solid symbols, while data taken at the maxima of the $\rho(H)$ curves are shown with open symbols.

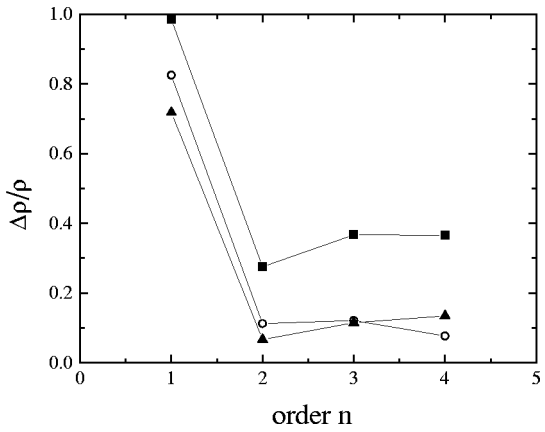

FIG. 9. $\Delta\rho/\rho$ as a function of matching field for the sample with 300-nm Ag dots for different applied current densities (■ 22, o 32, and ▲ 43 kA/cm^2).

Ni dots, which show clear matching effects for all current densities at all matching field [see Fig. 4(a)], and they are also different from the $j(V)$ curves for the samples with smaller Ni dots, which show no matching effects at low currents and two regions with different curvatures [see Fig. 4(b)].

The difference between the first and the higher-order matching fields can additionally clearly be observed in the normalized change of the resistivity $\Delta\rho/\rho$ at each matching field. This is shown in Fig. 9 for the sample with 300-nm Ag dots as a function of various current densities. Similar to the data shown before, the first-order matching peak is much more pronounced than the peaks for the higher orders. Figure 9 shows again that the periodic pinning is different from the samples with Ni dots. For the higher-order matching fields $(n>1)$ $\Delta\rho/\rho$ is approximately constant for the samples with Ag dots, while it decreases monotonically for the sample with 340-nm Ni dots [see Fig. 5(a)] and it goes through a maximum for the samples with smaller Ni dots [see Fig. 5(b)].

As mentioned above, the periodic pinning with the Ag dots seems to be less pronounced than for the samples with Ni dots. To show this more quantitatively we plot in Fig. 10 the highest order n_{max} of matching peak observed in the $\rho(H)$ measurements vs the dot diameter for the Ni (solid symbols) and Ag dots (open symbols), respectively. For all samples n_{max} is always larger for the Ni dots than for the Ag dots. This shows conclusively that the magnetic dots pin the vortices in the Nb more effectively than the nonmagnetic dots.

B. Discussion

The observed matching effects for samples with Ag dots suggest that the corrugation of the Nb film may not be negligible and can give rise to vortex pinning. A similar result was also obtained by M. Van Bael, who showed similar matching effects for Pb films deposited on top of either nonmagnetic metallic or semiconducting dots.[31] The corrugation may lead to a pinning of the vortices due to an effectively reduced thickness of the superconducting thin film around the perimeter of the dot. This reduced thickness can pin a vortex since the loss in condensation energy due to the nor-

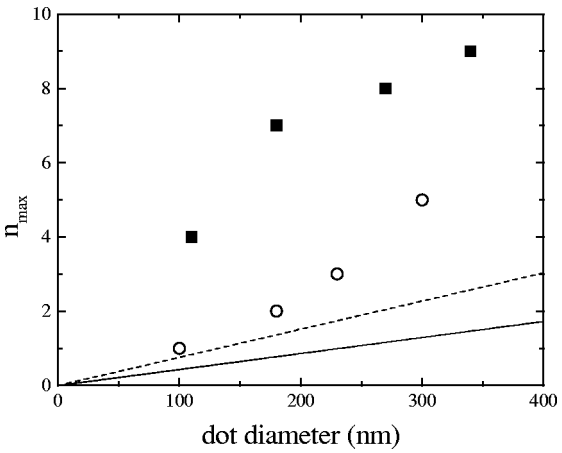

FIG. 10. Highest order n_{max} of observed matching peaks in $\rho(H)$ as a function of dot diameter for samples with Ag (o) and Ni (■) dots. The saturation number n_s [given by Eq. (2)] is indicated for $\xi=58$ nm (corresponding to $T/T_c=0.98$, solid line) and $\xi=33$ nm (corresponding to $T/T_c=0.94$, dashed line).

mal conducting vortex core is minimized, if the vortex is positioned at the constriction of the superconducting film. Furthermore, it is well known that in superconducting thin films the critical temperature can decrease with decreasing thickness and the Nb film used in this paper have thicknesses where this effect becomes important.[32–34] Thus the corrugation of the Nb film may also locally suppress superconductivity along the perimeter of the dot. The above discussed pinning mechanism would suggest that any pinning due to the corrugation will be diminished for thicker superconducting films, when the ratio of the film thickness to dot thickness increases. Indeed measurements on similar samples with Ag dots and a larger Nb film thickness (1000 Å) showed no periodic pinning effects, even though for samples with the same Nb thickness and magnetic dots the periodic pinning effects still persisted.[26]

Although there are periodic pinning effects for the samples with nonmagnetic dots, the comparison of the data for samples with Ni and Ag dots (Fig. 10) shows that the periodic pinning effects are more pronounced for the samples with magnetic dots. This, of course, opens up the question about the role of the magnetism for the vortex pinning. It has been suggested early on that the stray field of the magnetic dots can locally suppress superconductivity and thus lead to vortex pinning.[7,9] However, the measurements presented in this paper are independent of magnetic history and show no hysteresis effects. This suggests that the influence of the stray field is negligible. This is in contrast to results obtained by several different groups.[7,9,13] One possibility to resolve this discrepancy is that the dots in this work are significantly smaller than the ones used in earlier studies and that due to their smaller volume (approximately 100 times smaller compared to Ref. 7 and five times smaller compared to Ref. 9) the stray field is of less importance. Also in Ref. 13 the dots are potentially magnetized out-of-plane, which can give strong hysteresis effects due to a direct interaction of the magnetic fields of the vortices with the dot magnetization. This is in contrast to our experiments where the shape anisotropy of the dots suggests that the magnetization is in the plane of the superconducting film at moderate magnetic fields. Other possible pinning mechanisms due to the magnetism of the dots are either a gain in magnetic energy by aligning the vortices with the magnetic dots, or a local suppression of superconductivity due to a proximity effect between the superconducting thin film and the ferromagnetic dot.

In Fig. 10 we showed that the highest order n_{max} of matching fields varies with dot diameter for samples with Ni and Ag dots. Since n_{max} is equivalent to the number of vortices per pinning center it is interesting to compare this number to the so-called saturation number n_s given by[35]

$$n_s=\frac{d}{4\xi(T)}. \tag{2}$$

This saturation number gives the maximum number of vortices that fit into an insulating inclusion with a diameter d and is determined from solving the London equations for a superconductor with a single cylindrical hole.[35] It should be noted, however, that the validity of this expression may not necessarily be easily extended to a situation with periodic arrays of pinning centers, since the interaction between neighboring pinned vortices may become important.[20] Nevertheless, we show in Fig. 10 the saturation number n_s as a function of dot diameter for $\xi=33$ nm and $\xi=58$ nm (dashed and solid lines, respectively). These are the upper and lower limits for the coherence length for the various measurement temperatures at which the data for Fig. 10 was taken. For both the Ni dot and Ag dot samples n_{max} always exceeds n_s. This suggests, that at the higher-order matching field there are always vortices, which are not pinned at the dots, but at interstitial positions. Such vortex arrangements with interstitials have been observed experimentally[11] and subsequently reproduced in numerical simulations.[16]

The presence of interstitial vortices should give rise to a distinctively different pinning properties at the first and higher-order matching fields.[36] Experimentally, a clear difference between the first and the higher-order matching peaks is observed for the samples with Ag dots (see Fig. 9). Indeed the resistivity change $\Delta\rho/\rho$ is bigger for the first matching field than for the higher-order matching field. Also notice that the critical current density drops rapidly after the first matching field (see Fig. 8). This is consistent with a vortex lattice with weaker pinned interstitial vortices. By contrast the samples with Ni dots show no clear difference between the first and the higher-order matching field in the resistivity change (see Fig. 5).

Another possible way to distinguish between a situation with interstitial and multiquanta vortices is from the $j(V)$ curves for various magnetic fields.[36] If there are interstitial vortices present, they should be more weakly pinned than the vortices pinned at the dots. Thus with increasing current density first the interstitial vortices become depinned and then at higher currents the vortices at the periodic pinning centers also become depinned.[15,17] This gives rise to a ''kink'' in the $j(V)$ curves, which has been experimentally observed by E. Rosseel *et al.* for superconductors with regular arrays of holes.[36]

The samples with Ag dots show above the first matching field two different slopes in their $j(V)$ curves (see Fig. 8). Again, this is consistent with having interstitial vortices at

higher matching fields for these samples. On the other hand, for the samples with Ni dots the situation is not that clear. The samples with smaller Ni dots have $j(V)$ curves which show two very distinctive regimes [see Fig. 4(b)]. The two regimes even have opposite curvature. However, these two regimes are observed even for magnetic fields at or below the first matching field. This indicates, that in these samples the occurrence of two different behaviors separated by a clear kink in the $j(V)$ curves is independent of the presence of interstitial vortices. On the other hand, the samples with the 340-nm Ni dots show no crossover in their $j(V)$ curves [see Fig. 4(a)]. Thus while at higher matching fields the data for the samples with Ag dots is consistent with interstitial vortices, it remains unclear what the geometry of the vortex lattice is at higher matching fields for the samples with Ni dots.

V. CONCLUSION

In conclusion, we have shown periodic pinning as a function of pinning center size for Nb films with magnetic (Ni) dots and with nonmagnetic (Ag) dots. The samples with Ni dots show qualitatively different periodic pinning for very large Ni dots compared to smaller ones. This different behavior is clearly shown in the magnetic-field dependence of the critical current density, the $j(V)$ curves, and the resistivity changes $\Delta\rho/\rho$. Comparing the results to samples with Ni dots on an array with a larger lattice constant shows that this change in behavior is governed by the edge-to-edge separation of the Ni dots and therefore the size is not the determining factor. This can be explained by a crossover from a weak pinning regime (for large dot separations) to a superconducting wire network regime (for small dot separations).

Furthermore, the comparison between the samples with Ag and Ni dots show a more effective pinning for the samples with magnetic dots. This shows that even though corrugation of the Nb film may give rise to vortex pinning, there is also a magnetic contribution of the vortex pinning for the Ni dots. In addition, the magnetic-field dependence of the $j(V)$ curves and the resistivity changes $\Delta\rho/\rho$ indicates interstitial vortices at higher matching fields for the samples with Ag dots, while the geometry of the vortex lattice at higher matching fields remains unclear for the samples with Ni dots.

ACKNOWLEDGMENTS

We would like to acknowledge many useful discussions with Y. Bruynseraede, J. I. Martín, V. V. Moshchalkov, C. Reichhardt, J. Vicent, and G. Zimanyi. Also we would like to thank S. Kim for his assistance with the Nb deposition. One of us (P. Prieto) would like to thank the Guggenheim Foundation for supporting his stay at UCSD. This work was supported by DOE, AFOSR, and the UC-CLC program.

*Permanent address: Universidad del Valle, Cali, Colombia.

[1] A. M. Campbell and J. E. Evetts, Adv. Phys. **21**, 199 (1972).
[2] For an extensive review, see G. Blatter, M. V. Feigel'man, V. B. Geshkenbein, A. I. Larkin, and V. M. Vinokur, Rev. Mod. Phys. **66**, 1125 (1994).
[3] For a brief review, see G. W. Crabtree and D. R. Nelson, Phys. Today **50** (4), 38 (1997).
[4] O. Daldini, P. Martinoli, J. L. Olsen, and G. Berner, Phys. Rev. Lett. **32**, 218 (1974).
[5] A. T. Fiory, A. F. Hebard, and S. Somekh, Appl. Phys. Lett. **32**, 73 (1978).
[6] M. Baert, V. V. Metlushko, R. Jonckheere, V. V. Moshchalkov, and Y. Bruynseraede, Phys. Rev. Lett. **74**, 3269 (1995).
[7] Y. Otani, B. Pannetier, J. P. Nozières, and D. Givord, J. Magn. Magn. Mater. **126**, 622 (1993).
[8] J. I. Martín, M. Vélez, J. Nogués, and I. K. Schuller, Phys. Rev. Lett. **79**, 1929 (1997).
[9] M. J. Van Bael, K. Temst, V. V. Moshchalkov, and Y. Bruynseraede, Phys. Rev. B **59**, 14 674 (1999).
[10] J. I. Martín, M. Vélez, A. Hoffmann, I. K. Schuller, and J. L. Vicent, Phys. Rev. Lett. **83**, 1022 (1999).
[11] K. Harada, O. Kamimura, H. Kasai, T. Matsuda, A. Tonomura, and V. V. Moshchalkov, Science **274**, 1167 (1996).
[12] J.-Y. Lin, M. Gurvitch, S. K. Tolpygo, A. Bourdillon, S. Y. Hou, and J. M. Phillips, Phys. Rev. B **54**, 12 717 (1996).
[13] D. J. Morgan and J. B. Ketterson, Phys. Rev. Lett. **80**, 3614 (1998).
[14] C. Reichhardt, J. Groth, C. J. Olson, S. B. Field, and F. Nori, Phys. Rev. B **54**, 16 108 (1996).
[15] C. Reichhardt, C. J. Olson, and F. Nori, Phys. Rev. Lett. **78**, 2648 (1997).
[16] C. Reichhardt, C. J. Olson, and F. Nori, Phys. Rev. B **57**, 7937 (1998).
[17] C. Reichhardt, C. J. Olson, and F. Nori, Phys. Rev. B **58**, 6534 (1998).
[18] C. Reichhardt and F. Nori, Phys. Rev. Lett. **82**, 414 (1999).
[19] A. Bezryadin and B. Pannetier, J. Low Temp. Phys. **102**, 73 (1996).
[20] V. V. Moshchalkov, M. Baert, V. V. Metlushko, E. Rosseel, M. J. Van Bael, K. Temst, R. Jonckheere, and Y. Bruynseraede, Phys. Rev. B **54**, 7385 (1996).
[21] V. V. Moshchalkov, M. Baert, V. V. Metlushko, E. Rosseel, M. J. Van Bael, K. Temst, Y. Bruynseraede, and R. Jonckheere, Phys. Rev. B **57**, 3615 (1998).
[22] N. Takezawa and K. Fukushima, Physica C **228**, 149 (1994).
[23] N. Takezawa and K. Fukushima, Physica C **290**, 31 (1997).
[24] A. Hoffmann, Ph.D. thesis, University of California–San Diego, 1999.
[25] J. I. Martín, Y. Jaccard, A. Hoffmann, J. Nogués, J. M. George, J. I. Vicent, and I. K. Schuller, J. Appl. Phys. **84**, 411 (1998).
[26] Y. Jaccard, J. I. Martín, M.-C. Cyrille, M. Vélez, J. L. Vicent, and I. K. Schuller, Phys. Rev. B **58**, 8232 (1998).
[27] C. Kittel, *Introduction to Solid State Physics*, 7th ed. (Wiley, New York, 1996).
[28] B. Pannetier, J. Chaussy, R. Rammal, and J. C. Villegier, Phys. Rev. Lett. **53**, 1845 (1984).
[29] W. A. Little and R. Parks, Phys. Rev. A **133**, A97 (1964).
[30] S. Bhattacharya and M. J. Higgins, Phys. Rev. Lett. **70**, 2617 (1993).
[31] M. Van Bael, Ph.D. thesis, Katholieke Universiteit Leuven, Belgium, 1998.
[32] A. F. Mayadas, R. B. Laibowitz, and J. J. Cuomo, J. Appl. Phys. **34**, 1287 (1972).

[33] S. A. Wolf, J. J. Kennedy, and M. Nisenoff, J. Vac. Sci. Technol. **13**, 145 (1976).

[34] I. Banerjee and I. K. Schuller, J. Low Temp. Phys. **54**, 501 (1984).

[35] G. S. Mkrtchyan and V. V. Schmidt, Zh. Éksp. Teor. Fiz. **61**, 367 (1972) [Sov. Phys. JETP **34**, 195 (1972)].

[36] E. Rosseel, M. Van Bael, M. Bart, R. Jonckheere, V. V. Moshchalkov, and Y. Bruynseraede, Phys. Rev. B **53**, 2983 (1996).